Clustering within rootless cone groups on Iceland and Mars: Effect of nonrandom processes

B. C. Bruno,[1] S. A. Fagents,[1] T. Thordarson,[2] S. M. Baloga,[3] and E. Pilger[1]

Received 29 March 2004; revised 14 May 2004; accepted 10 June 2004; published 27 July 2004.

[1] This study aims at quantifying the spatial distribution of cones within rootless cone groups (RCGs). Our data set consists of (1) seven Icelandic RCGs (identified through field investigations), (2) seven candidate RCGs on Mars (identified through Mars Orbiter Camera (MOC) and Thermal Emission Imaging System (THEMIS) images), and (3) four groups of impact craters on Mars (also identified through MOC and THEMIS images) to determine if they can be remotely distinguished from the RCGs purely on the basis of their spatial distribution. Several independent statistical techniques are used, including nearest neighbor analysis, analysis of variance (ANOVA), and linear alignment detection analysis. Our results indicate that the spatial distribution of each RCG is not random: Within a cone group, cones preferentially form near existing cones. The presence of at least one significant linear cone alignment in each RCG (and strong linear alignments in some groups) suggests that rootless cones form as the surface signature of preferred lava pathways. An ANOVA on mean nearest neighbor distances reveals the Martian cone groups to be statistically indistinguishable from the Icelandic RCGs, supporting existing interpretations that they represent rootless cone groups. A similar ANOVA showed that the Martian cone groups do not resemble the Martian impact crater clusters studied: The impact craters have significantly greater nearest neighbor distances and show no evidence of aggregation within a crater group. *INDEX TERMS:* 8414 Volcanology: Eruption mechanisms; 8450 Volcanology: Planetary volcanism (5480); 8499 Volcanology: General or miscellaneous; 6225 Planetology: Solar System Objects: Mars; 5480 Planetology: Solid Surface Planets: Volcanism (8450); *KEYWORDS:* rootless cones, Iceland, hydrovolcanic, pseudocraters, nearest neighbor, nonrandom

Citation: Bruno, B. C., S. A. Fagents, T. Thordarson, S. M. Baloga, and E. Pilger (2004), Clustering within rootless cone groups on Iceland and Mars: Effect of nonrandom processes, *J. Geophys. Res.*, *109*, E07009, doi:10.1029/2004JE002273.

1. Introduction

[2] Icelandic rootless cones (or pseudocraters) are hydrovolcanic cones of spatter and scoria that rest directly on compound pahoehoe lava flows (Figure 1). They form as a result of explosive interaction between a flowing lava and the underlying waterlogged substrate [*Thorarinsson*, 1951, 1953]. They are typically stratified (formed by multiple eruptive events), inversely size graded (showing decreasing explosivity with time), and capped with welded spatter (indicating cessation of explosivity due to volatile depletion) [*Thordarson*, 2000]. Some cones have multiple craters. As the activity at a given cone subsides, explosions are typically initiated elsewhere, forming a group of tens to hundreds of cones within the flow field.

[3] A schematic of rootless cone formation is shown in Figure 2. First, tube-fed lava is laterally injected through preferred lava pathways, causing local lava inflation and subsequent subsidence. As the lava sinks into the underlying sediment, cracks develop in the basal lava crust, initiating contact (and explosive interaction) between the lava and the waterlogged sediment. This explosive event precludes further lava flow movement (and therefore further rootless cone formation) in the downflow direction. However, rootless cones may form upflow, as continued inflation and subsidence cause new cracks to develop upflow.

[4] The spatial distribution of rootless cones within a cone group varies considerably. In some groups the cones appear to be linearly aligned, suggesting a possible correlation with underground lava tubes (or preferred lava pathways). In other groups, however, cones appear to be more or less randomly distributed. This paper investigates several Icelandic rootless cone groups (RCGs) in order to (1) characterize the spatial distribution of cones (i.e., the degree of randomness) in different geologic settings, (2) relate the spatial distribution to the underlying physical processes and controls governing cone distribution (especially the relative roles of lava tube distribution and substrate hydrology), and (3) develop a remote sensing methodology for discriminating RCGs on Earth and other planets where in situ investigation is not possible. Remote identification of rootless cones (i.e., distinguishing them from other conical

[1]Hawaii Institute of Geophysics and Planetology, University of Hawaii at Manoa, Honolulu, Hawaii, USA.
[2]Department of Geology and Geophysics, University of Hawaii at Manoa, Honolulu, Hawaii, USA.
[3]Proxemy Research, Bowie, Maryland, USA.

0148-0227/04/2004JE002273

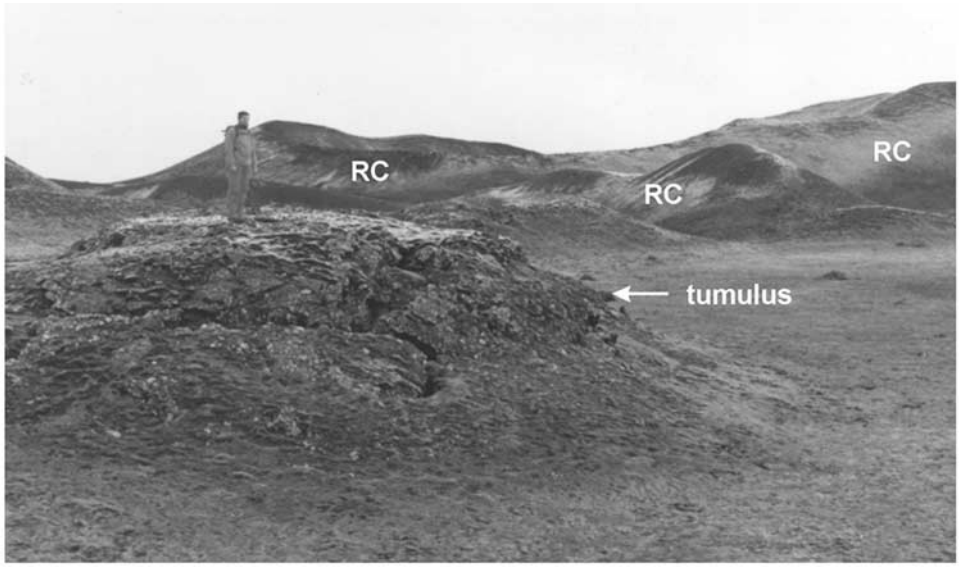

Figure 1. Field photograph of Innri Eyrar, a rootless cone group associated with the Laki 1783–1784 lava flow in south central Iceland. Rootless cones (RC) and tumulus are labeled.

features), however, is not straightforward, and, to some extent, we must rely on the geological context. Of particular interest is Mars, where potential RCGs have been identified (Figure 3). Although the proposed Martian cones are typically an order of magnitude wider than the Icelandic rootless cones, this is expected for the same starting conditions because of planetary differences. The lower Martian atmospheric pressure enables greater gas expansion, greater eruption velocities, and lower particle drag forces, and the lower Martian gravity enables clastics to stay aloft for a longer period of time [*Greeley and Fagents*, 2001; *Fagents et al.*, 2002; *Fagents and Thordarson*, 2004]. If confirmed, the existence of rootless cones on Mars would provide an important diagnostic for the presence of near-surface water or ice and its evolution over time.

[5] Our approach is to apply several statistical methods to characterize the spatial distribution of cones within a cone group, including nearest neighbor analysis, analysis of variance (ANOVA) on the nearest neighbor results, and a linear alignment detection analysis. We find that the Icelandic RCGs show a significant departure from a random spatial distribution, and we provide suggestions for the process(es) that may be responsible for this departure from randomness. To demonstrate how our approach can be applied using only remote sensing data, we apply our methodology to candidate RCGs on Mars, where the geologic context, although highly constrained, is not completely unambiguous. Here we find that the Martian cone groups are statistically indistinguishable from the Icelandic RCGs, thus supporting existing morphologic interpretations of these cone fields and the existence of near-surface ground ice.

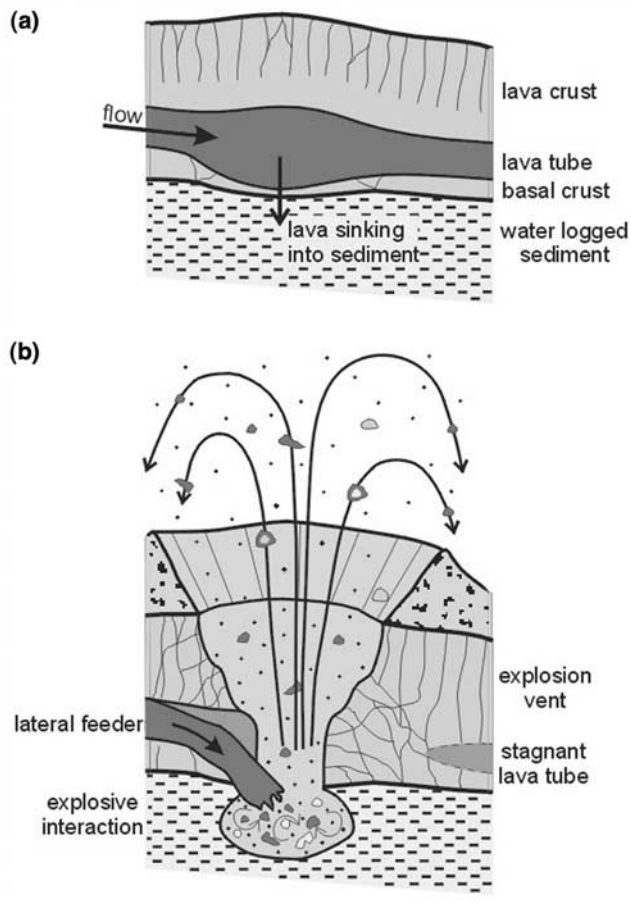

Figure 2. Schematic of rootless cone formation. (a) Tube-fed lava sinks into the underlying sediment, causing cracks in the basal crust and initiating explosive interaction with the waterlogged sediment. (b) This explosive event precludes further downflow lava movement; new rootless cones can only form upflow.

2. Data

2.1. Icelandic Rootless Cone Groups

[6] Three data sets are used in this analysis. First, we analyze seven RCGs from three lava flow fields (Laki, Eldgja, and Leitin) in south central Iceland from stereo air

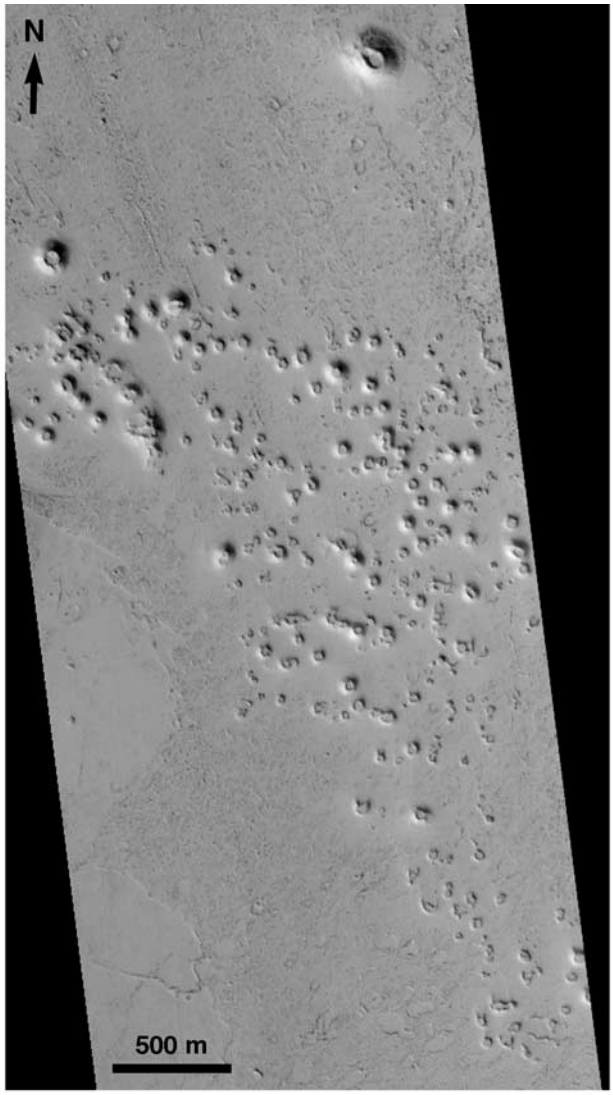

Figure 3. Candidate rootless cone group located ~400 km west of Amazonis Planitia, Mars (southern portion of MOC image M0801962, centered at 25.9°N, 170.3°E). Illumination is from the lower left.

photographs (Table 1); a location map is given in Figure 4. These rootless cones have been previously identified as hydrovolcanic features by numerous workers on the basis of detailed field investigations [*Thoroddsen*, 1894; *Thorarinsson*, 1951, 1953]. Any ambiguity as to whether a given feature in a rootless cone group was indeed a cone was resolved using stereo air photographs. Cone morphology and spatial density vary considerably among these RCGs, with cone diameters and heights in the ranges of 5–450 m and 2–40 m, respectively [*Thordarson et al.*, 1992; *Thordarson and Hoskuldsson*, 2002].

2.2. Martian Candidate Rootless Cone Groups

[7] Second, we consider seven candidate RCGs on Mars in areas previously identified as potentially hydrovolcanic from early Viking images [*Frey et al.*, 1979; *Allen*, 1980; *Frey and Jarosewich*, 1982; *Hodges and Moore*, 1994]. We analyze the spatial distribution of cones within these groups on the basis of high-resolution data acquired by the Mars Orbiter Camera (MOC) aboard the Mars Global Surveyor spacecraft, as well as the more recent Thermal Emission Imaging System (THEMIS) on the Mars Odyssey mission. Image resolutions are in the range of 4.5–19 m/pixel (Table 2). These cone groups are all located in the northern lowland plains at middle to low latitudes (Figure 5).

[8] How did we remotely identify these candidate RCGs? As a starting point, we adopted the criteria of previous workers, including (1) distinct positive-relief features with conical form, (2) location on lava flow surfaces or volcanic plains, and (3) lack of association with eruptive fissures [*Thordarson*, 2000; *Greeley and Fagents*, 2001; *Fagents et al.*, 2002; *Fagents and Thordarson*, 2004]. We then developed and applied further criteria to minimize the likelihood that irregular terrain would be mistakenly interpreted for rootless cones. First, we considered only cones either with visible craters or of a similar size to cones with visible craters (i.e., conical features that were too small for craters to be resolved were excluded). Elongate positive-relief features were included only if multiple craters were visible. In all cases, cones were required to stand out clearly against the background topography; cones on hummocky terrain were avoided.

2.3. Martian Impact Crater Groups

[9] Another feature commonly appearing in clusters on the Martian surface is impact craters. It has been suggested that the Martian candidate RCGs may not be cone groups at all but instead clusters of impact craters whose positive topographic relief is due to resistant ejecta deposits which armor surfaces undergoing wind erosion. Although wind erosion would likely produce a plateau rather than a cone, and although there is little or no evidence for wind erosion in these images [*Lanagan et al.*, 2001], we nevertheless consider the possibility that these constructs may have an impact origin. Thus we examined four groups of impact craters on Mars (Figure 5), again from MOC and THEMIS images, to see if they could be remotely differentiated from RCGs exclusively on the basis of their spatial distribution. On the basis of their clustering, these nonvolcanic craters are interpreted to represent either secondary impacts (formed by the ejection of debris that was itself ejected

Table 1. Rootless Cone Groups in Iceland [after *Fagents and Thordarson*, 2004]

Lava Flow	Age	Volume, km^3	Length, km	Rootless Cone Group (RCG)	RCG Area, km^2	Aerial Photo Scale
Laki	1783–1784	15.1	55	Blagil	<1	1:37000
Laki	1783–1784			Innri Eyrar	1.1	1:37000
Laki	1783–1784			Hnuta	1	1:37000
Laki	1783–1784			Trollhamar	1.5	1:37000
Laki	1783–1784			Stakafell	0.7	1:37000
Eldgja	1.1 kyr B.P.	14.2	60	Landbrot	150	1:37000
Leitin	4.6 kyr B.P.	3	35	Raudholar	1.2	1:16000

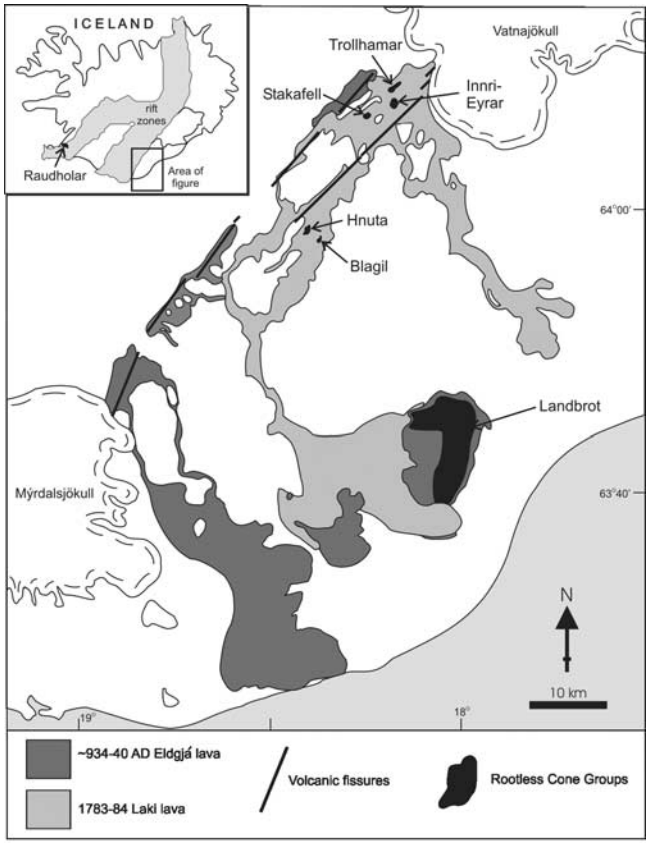

Figure 4. Location map of Icelandic rootless cone groups.

from a nearby impact) or simultaneous impact by many pieces of a larger meteor that broke up upon entry into the Martian atmosphere (Figure 6).

[10] For all three data sets we include only groups with at least 60 data points (i.e., cones or craters) to obtain an adequate sample size for statistical analysis. Although this minimum threshold is somewhat arbitrary, tests on randomly generated synthetic images with less than 50 or 60 points revealed inconsistent (i.e., not necessarily random) results.

3. Methodology

3.1. Nearest Neighbor Analysis

[11] We invoke "nearest neighbor" methodology to assess the degree of spatial randomness within a cone field and to evaluate the statistical confidence in this assessment. For detailed information on this method (including the underlying equations and their derivations), the reader is directed to *Clark and Evans* [1954]. Briefly, this technique (which requires that each cone be represented by a point) quantifies the characteristic spacing between nearest neighbors within a given spatial area and compares this spacing to that expected of a random (Poisson) distribution. The key parameters are R (the ratio of the mean actual distance between a point and its nearest neighbor to that of a Poisson distribution) and c (a confidence estimate in the departure from randomness). At the 0.05 significance level the critical value of c is 1.96 (i.e., c will exceed 1.96 in a Poisson distribution 5% of the time).

[12] Figure 7 illustrates the nearest neighbor technique on synthetic images [*Bruno et al.*, 2004]. Randomly distributed cones would be expected to have $R \sim 1$ (i.e., the actual nearest neighbor distance approximates that expected of a Poisson distribution) and $c < 1.96$ (i.e., no significant departure from randomness). This suggests that cones form independently of one another, neither attracted to nor repelled by previously formed cones (Figure 7a). Small R values ($R < 1$) indicate aggregation within a cone group (i.e., the cones are closer together than would be randomly expected), indicating that cones preferentially form near existing cones. If substrate hydrology is controlling this nonrandom behavior, highly localized volatile depletion during cone formation (to allow another cone to form nearby) and/or variable volatile abundance throughout the cone field is suggested. Alternatively, the clustering may indicate preferential formation along a single (or bifurcating) lava pathway (Figure 7b). An R value exceeding unity indicates that cones tend to form away from existing cones, with uniform distributions (i.e., maximum spacing) having maximum R. *Clark and Evans* [1954] have shown that for infinitely large uniform distributions, R reaches a maximum value of $\sim$2.15; R can be slightly greater for finite uniform distributions. In this case, cones would preferentially form away from existing cones, suggesting (1) uniform lava supply throughout the cone field, (2) uniform volatile abundance throughout the cone field, and (3) significant volatile depletion associated with the formation of a given rootless cone, preventing other cones from forming nearby (Figure 7c).

[13] An advantage of nearest neighbor analysis over classical distribution fitting (e.g., running a chi-square goodness of fit test to a Poisson or uniform distribution)

Table 2. Candidate Rootless Cone Groups and Impact Crater Groups on Mars

Candidate RCGs	Image	Location of Image Center	Resolution, m/pixel
West of Amazonis Planitia 1	Southern part of MOC m0801962	25.9°N, 170.3°E	4.5
West of Amazonis Planitia 2	Northern part of MOC m0801962	25.9°N, 170.3°E	4.5
Cerberus Plains 1 (southernmost of 3 RCGs)	Southern part of MOC m0800090	2.7°N, 143.9°E	5.8
Cerberus Plains 2 (central of 3 RCGs)	Southern part of MOC m0800090	2.7°N, 143.9°E	5.8
Cerberus Plains 3 (northernmost of 3 RCGs)	Southern part of MOC m0800090	2.7°N, 143.9°E	5.8
Acidalia Planitia	Northern part of THEMIS V05393016	40.3°N, 353.1°E	19
Isidis Planitia	THEMIS V06251019	11.6°N, 84.8°E	18
	Impact Crater Groups		
Acidalia Planitia	Northern part of THEMIS V05393016	40.3°N, 353.1°E	19
Ares/Tiu Valles	MOC 2-552, released 22 Nov. 2003	19.9°N, 326.7°E	13
Nili Fossae	Central part of THEMIS I02394009	20.5°N, 76.2°E	100
South Isidis Planitia	Northern part of THEMIS V01033003	3.9°N, 85.5°E	18

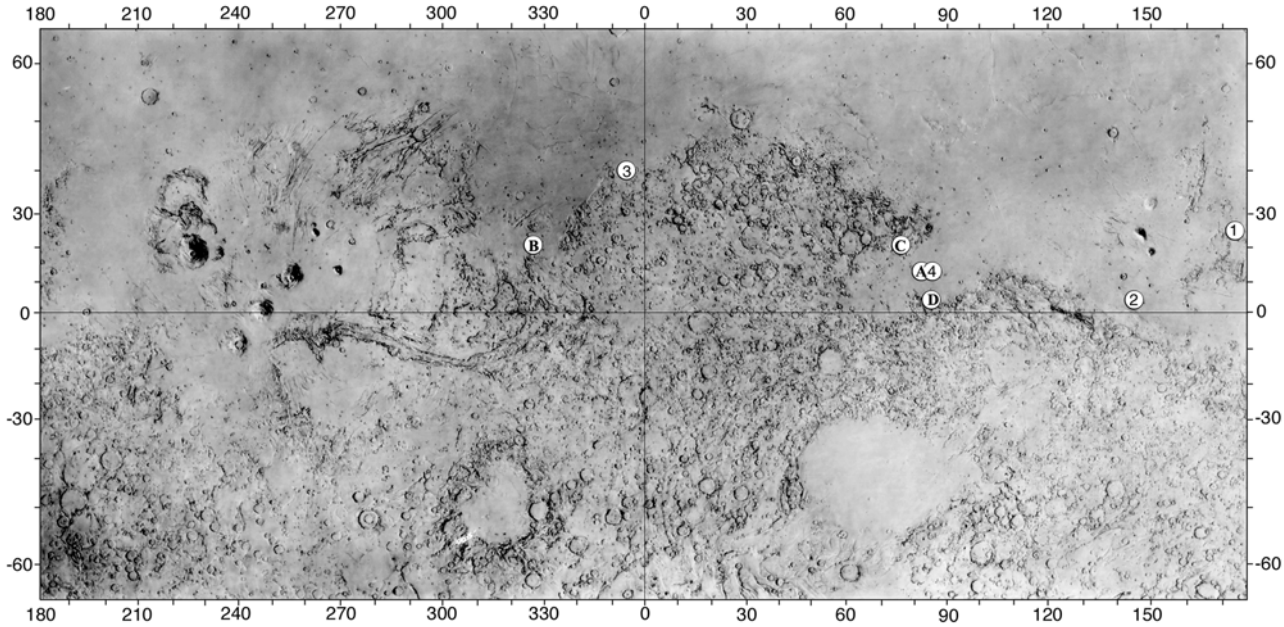

Figure 5. Location map of Martian candidate rootless cone groups: 1, ~400 km west of Amazonis Planitia (two groups); 2, Cerberus Plains (three groups); 3, Acidalia Planitia; and 4, Isidis Planitia. Also shown are the locations of impact crater clusters: A, Acidalia Planitia; B, Ares/Tiu Valles; C, Nili Fossae; and D, S. Isidis Planitia.

is that there is no arbitrary selection of bins, the choice of which can significantly affect results. However, the nearest neighbor technique is sensitive to area selection, as the expected nearest neighbor distance from a Poisson distribution is predicated on the point density (number of points per unit of area). Any empty space surrounding the cone group will increase the random distance estimate, decreasing R and preferentially indicating clustering. It is therefore essential to systematically apply an area selection procedure to minimize the area surrounding the cone group. There are several area selection options to choose from, such as (1) fitting an external rectangle to the cone group so as find the minimum area that encompasses the entire cone group; (2) fitting an internal rectangle to the cone group so as to find the maximum area that is fully contained by the cone group; or (3) fitting shapes other than rectangles (e.g., ovals) to the cone group, either externally or internally. We have found that although the choice of area selection method does affect the R value (e.g., choosing an internal shape results in higher R), the effect is systematic so as not to affect comparisons among cone groups. Therefore any of these area selection procedures can be used, provided it is systematically applied.

[14] Our protocol involves (1) rotating the image through 1° increments to find the minimum rectangular area that encompasses the entire cone group, (2) recording the (rotated) coordinates of the centerpoint of the crater atop each cone (or, in cases where the crater is not visible, in the center of the cone), (3) checking the coordinates for errors (e.g., duplication), and (4) performing the nearest neighbor analysis. Our data sets are sufficiently small that the distance between each pair of points can be calculated, and the minimum (i.e., the nearest neighbor) distance can be determined without resorting to sector analysis [*Clark and Evans*, 1954].

[15] Nearest neighbor analysis determines randomness exclusively on the basis of the distance between points; it does not consider their relative orientation. Thus points in perfect linear alignment, with a mean spacing approximating that of a Poisson distribution with the same point density, will be interpreted as random. It is therefore necessary to apply a second technique to detect any linear alignments in the data.

3.2. Linear Alignment Detection Analysis

[16] Both in the field and in aerial photographs, several of the RCGs (e.g., Landbrot) appear to display pronounced linear alignments of cones (Figure 8). The significance of these apparent alignments is unclear but might be related to sequential explosions along preferred internal pathways (e.g., lava tubes). We are interested in determining whether these apparent trends are statistically significant or are simply an expected product of a random spatial distribution. Our approach is first to divide the entire cone group into subgroups on the basis of a separation distance (S). Our process of determining S is explained below, but to illustrate our method, let us assume $S = 5$ pixels. The first (i.e., upper leftmost) cone in the RCG is called the "starting cone" and is used to build the first subgroup. All cones located within 5 pixels of this starting cone are added to the first subgroup and are collectively called "first subgroup cones." We now iterate the process: All cones located within 5 pixels of any of these first subgroup cones are added to the list of first subgroup cones. We continue iterating this process until there are no more cones to add to the first subgroup (i.e., when all cones not in the first subgroup are greater than 5 pixels away from any cone in the first subgroup). At this point we start a second subgroup and repeat the process. Note that (1) all subgroups are required to contain a minimum of five cones, and (2) if every cone in a given

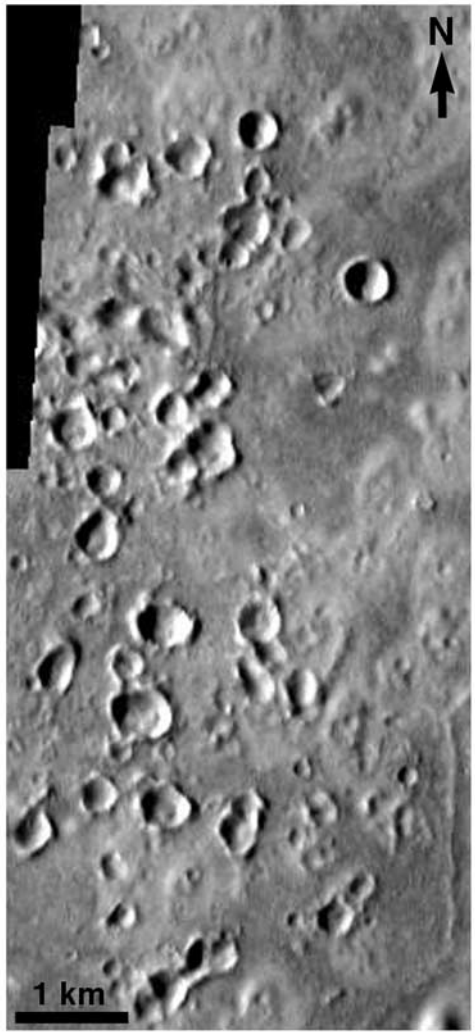

Figure 6. Impact crater cluster in Acidalia Planitia, Mars (northern portion of THEMIS V05393016, centered at 40.3°N, 353.1°E). Illumination is from the left. The craters represent either secondary craters or simultaneous impact by many pieces of a larger meteor that broke up prior to impact.

RCG is within 5 pixels of its nearest neighbor, the entire cone group would comprise only one subgroup.

[17] Once the subgroups are determined, the cones within each subgroup are fit with a least squares regression line. The significance of the linear correlation of each regression line is determined by comparing the calculated Pearson correlation coefficient (r) to the critical value for the given number of data points at the 0.05 level. The significance should be interpreted as follows: In the absence of a linear correlation, there is a 5% chance that the absolute value of r will nevertheless exceed the critical value. Our linear alignment detection analysis outputs both the number of cone subgroups with significant linear correlations (C_{sig}) and the number of subgroups with "strong" linear correlations ($C_{0.95}$), defined as having $r^2 > 0.95$. Figure 9a demonstrates this technique on a synthetic image.

[18] As noted above, the choice of S determines how the RCG is divided into subgroups: The smaller the choice of S, the greater the number of subgroups. To arrive at the optimal S for a given RCG, we first determine the mean actual distance (R_a) between each cone and its nearest neighbor. R_a is proportional to R, but it is not scaled by the mean nearest neighbor distance of a Poisson distribution. (Thus R_a has units of pixels, whereas R is dimensionless.) We then perform the linear alignment detection analysis for all values of S within 2 standard deviations of R_a and construct a histogram of the number of significant fits as a function of S. The minimum possible value of S is 1 pixel, indicating adjacent points. The optimal S corresponds to the maximum number of significant fits; correlation coefficients are used to break any ties (Figure 9b).

4. Results

4.1. Nearest Neighbor Analysis Results

4.1.1. Icelandic Rootless Cone Groups

[19] Nearest neighbor analysis of the seven Icelandic RCGs (Table 3) yields low R (0.57–0.88, R_{mean} = 0.74). This indicates a high degree of aggregation: The distance between a cone and its nearest neighbor is, on average, only 74% of that expected from a random (Poisson) spatial distribution. All c values exceed 1.96, indicating that this departure from randomness is significant at the 0.05 level. This nonrandom behavior indicates that the location of cone formation is being systematically controlled, most likely by the underlying lava pathway geometry and/or by the substrate hydrology. (See section 5.)

4.1.2. Martian Candidate Rootless Cone Groups

[20] Nearest neighbor results for the seven Martian candidate RCGs mirror the Icelandic results. The R values range from 0.66 to 0.85 (R_{mean} = 0.73), similarly indicating aggregation. Again, high c values (all >1.96) indicate a significant departure from randomness at the 0.05 level. A one-way analysis of variance (ANOVA) on the R values shows no difference between the spatial distribution of the Martian and Icelandic cone groups. The ANOVA yielded a probability (p) value of 0.86, indicating that the R values are statistically indistinguishable at the 0.05 level and thereby supporting a rootless (hydrovolcanic) origin of the Martian cone groups.

4.1.3. Martian Impact Crater Groups

[21] We examined four groups of impact craters on Mars to see if they could be remotely differentiated from RCGs exclusively on the basis of their spatial distribution. Nearest neighbor analysis on these four crater groups resulted in R values ranging from 0.92 to 1.17; only the highest R value yielded $c > 1.96$. This indicates that the spacing between craters within these crater groups is random or, in the one case, significantly greater than random. In no case is there evidence of aggregation within a crater cluster. A one-way ANOVA on the R values of the impact crater groups versus the Martian candidate RCGs yields $p = 0.0002$, showing a significant difference at the 0.05 level. (Including the Icelandic RCGs with the Martian candidate RCGs similarly results in $p = 0.0001$.) This shows that impact crater clusters and RCGs can be remotely distinguished purely on the basis of their spatial distribution.

4.2. Linear Alignment Detection Analysis Results

[22] Linear alignment detection analysis was applied to both the Icelandic and Martian cone groups to determine

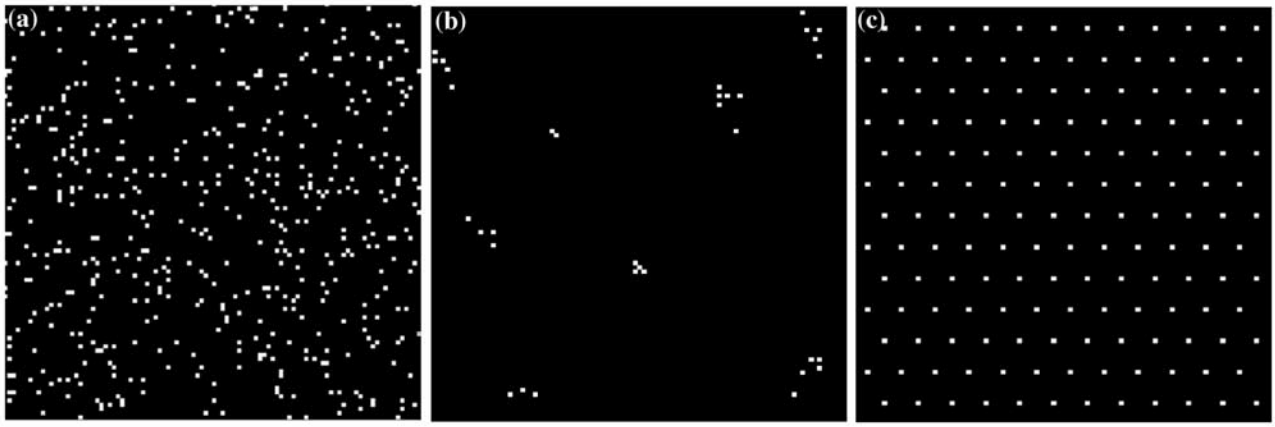

Figure 7. Illustration of the nearest neighbor technique on synthetic images. (a) Poisson distribution (R = 1.03, c = 1.27). Nearest neighbor distance is within the range expected from a random spatial distribution. Thus $R \sim 1$ and $c < 1.96$, indicating no significant departure from randomness. (b) Clustered distribution (R = 0.32, c = 7.62). Nearest neighbor distance is, on average, significantly less than would be expected from a random distribution ($R < 1$ and $c > 1.96$). (c) Uniform distribution (R = 2.19, c = 31.08). Nearest neighbor distance is at a maximum, significantly greater than would be expected from a random spatial distribution. Thus $R > 1$ and $c > 1.96$.

whether the apparent linear alignments of cones observed in some groups are statistically significant (Table 4). For the Icelandic RCGs this analysis yielded significant linear fits to at least one cone subgroup within each of the seven cone groups at the 0.05 level. The number of significant fits (C_{sig}) ranged from 1 to 23, with the number of strong linear correlations ($C_{0.95}$) ranging from 0 to 4. Linear trends appeared most strongly in the Landbrot cone group (Figure 10a); such alignments were largely absent in other cone groups such as Raudholar (Figure 10b).

[23] Linear alignment detection analysis for the Martian cone groups produced C_{sig} values ranging from 1 to 4 and $C_{0.95}$ values ranging from 0 to 1. These are the identical ranges of those Icelandic cone groups with $N <$ 600 (i.e., all Icelandic RCGs except Landbrot and Hnuta), again suggesting that the Martian groups are likely to be rootless cones.

5. Discussion

[24] Unlike the impact crater groups analyzed, all of the Icelandic and Martian cone groups studied indicate significant aggregation within a cone group. This intragroup aggregation indicates that some process (or processes) is systematically controlling the locations of cone formation within a cone group, thereby causing a departure from randomness. As rootless cones are formed by the explosive interaction of flowing lava and the underlying waterlogged substrate, the two likely controls are

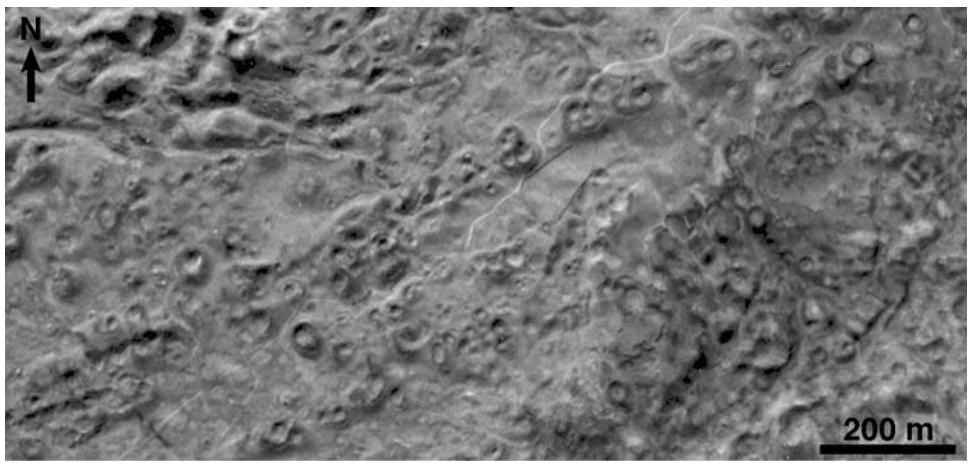

Figure 8. Aerial photograph of a portion of the Landbrot RCG. Illumination is from the upper left. Note the apparent linear alignments of cones trending NE–SW.

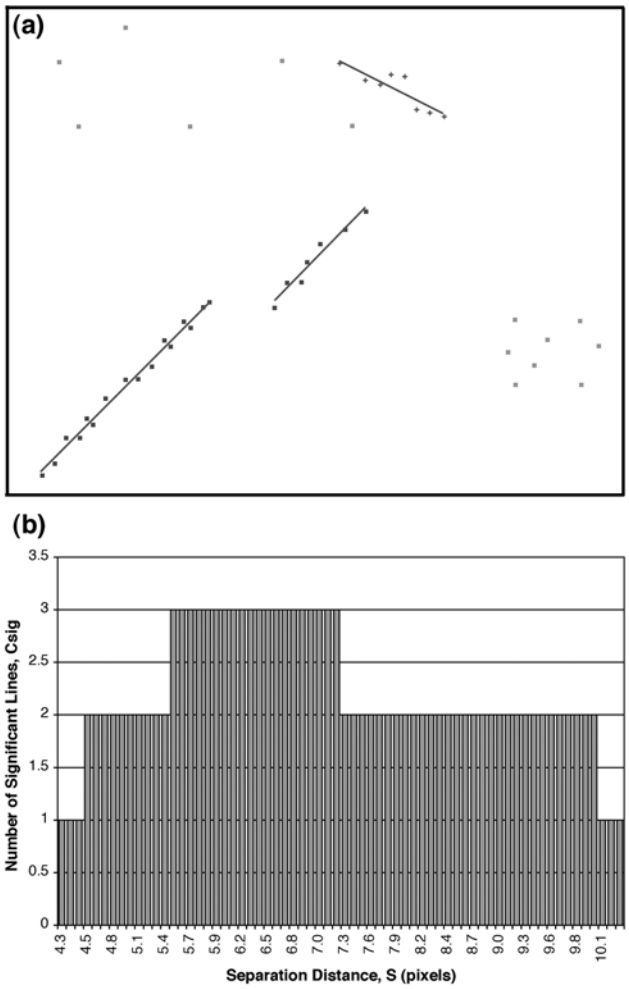

Figure 9. Illustration of linear alignment detection analysis on a synthetic image. (a) Four cone subgroups were determined using a separation distance (S) of 6 pixels. The three subgroups with significant linear correlations are fit with lines; cones in these subgroups are shown with either dark squares ($r^2 > 0.95$) or pluses ($r^2 < 0.95$). The remaining cones are represented by light squares. Cones have mean unscaled distance (R_a) of 4.0 pixels and standard deviation of 3.2 pixels. (b) Histogram showing the number of significant linear correlations as a function of separation distance (S), using S values within 2 standard deviations of R_a. The optimal S value corresponds to the maximum number of significant lines. Choosing S anywhere between 5.5 and 7.2 yields the maximum number of significant correlations (i.e., three) and the same combined r (not shown).

the substrate volatile abundance and the lava pathway distribution.

5.1. Lava Pathway Distribution as Controlling Factor on Rootless Cone Distribution?

[25] If the lava pathway distribution were the controlling factor, we would expect to see denser cone concentrations and quasi-linear alignments along preferred lava pathways. Linear alignment detection analysis revealed at least one significant linear alignment within each RCG and as many as 23 for Landbrot, four of which had strong linear correlations ($r^2 > 0.95$). Interestingly, these four lines are more or less parallel, trending from NNE to SSW (Figure 10a). We interpret these linear cone alignments as sequential cone formation along preferred pathways of lava flowing from the north-northeast. Strong correlations may suggest relatively narrow lava tubes. Future work includes detailed field investigations to map out lava tube systems within the cone groups. A similar subparallel arrangement of linear features is exhibited by one of the Cerberus cone groups (Figure 10c), although the linear correlations are weaker.

[26] An alternate approach to determining whether lava pathway geometry controls rootless cone distribution is to examine the spatial distribution of tumuli, that is, inflation features which form on pahoehoe flow fields by the continued injection of lava beneath a solid crust. Several workers have linked tumuli distribution to the underlying preferred lava pathways [*Guest et al.*, 1984; *Anderson et al.*, 1999; *Duncan et al.*, 2004], although other controls (such as topography) have been suggested [*Self et al.*, 1998]. In the context of this study, tumuli can be considered to be precursors to rootless cones, representing the first nonexplosive stage in cone formation.

[27] *Glaze et al.* [2004] observe a systematic clustering of tumuli in the Mauna Loa 1843 flow that results in linear alignment. *Duncan et al.* [2004] similarly note linearly aligned tumuli in the 1983 Mt. Etna flow. These studies support the argument that linear cone alignments represent the surface signature of well-defined lava tubes, topographic control, or preferred pathways for subsurface lava distribution. However, *Glaze et al.* [2004] also examined two other tumulus fields in Hawaii and Iceland with more or less random spatial distributions. In these tumulus fields the existence of lava tubes or preferred pathways was randomized by temporal changes in the lava distribution and

Table 3. Results of Nearest Neighbor Analysis[a]

	N	R	c
Iceland RCGs			
Blagil	87	0.87	2.40
Innri Eyrar	80	0.80	3.49
Hnuta	660	0.68	15.54
Landbrot	1282	0.77	15.53
Trollhamar	131	0.57	9.46
Stakafell	192	0.64	9.59
Raudholar	198	0.88	3.25
Mars Candidate RCGs			
West of Amazonis Planitia 1	125	0.85	3.16
West of Amazonis Planitia 2	282	0.84	5.10
Cerberus Plains 1	161	0.66	8.24
Cerberus Plains 2	90	0.67	6.06
Cerberus Plains 3	103	0.70	5.77
Acidalia Planitia	386	0.71	10.72
Isidis Planitia	247	0.69	9.19
Mars Impact Craters			
Acidalia Planitia	67	1.12	1.83
Ares/Tiu Valles	197	1.17	4.50
Nili Fossae	88	1.10	1.83
South Isidis Planitia	94	0.92	1.54

[a] N, number of cones or craters; R, ratio of the mean nearest neighbor distance to that expected of a Poisson distribution; c, statistical confidence in the departure from randomness ($c > 1.96$ indicates result is significant at the 0.05 level).

Table 4. Results of Linear Alignment Detection Analysis[a]

	N	R_a	SD	S	C_{sig}	$C_{0.95}$
			Iceland RCGs			
Blagil	87	44	22	54	4	1
Innri Eyrar	80	115	130	180	2	0
Hnuta	660	32	18	62	12	0
Landbrot	1282	20	13	29	23	4
Trollhamar	131	27	28	32	3	0
Stakafell	192	13	9	16	4	1
Raudholar	198	24	13	23	1	0
			Mars Candidate RCGs			
West of Amazonis Planitia 1	125	20	10	38	2	0
West of Amazonis Planitia 2	282	26	16	26	1	0
Cerberus Plains 1	161	14	11	20	4	0
Cerberus Plains 2	90	18	11	17	1	0
Cerberus Plains 3	103	23	16	27	2	0
Acidalia Planitia	386	10	5	12	2	0
Isidis Planitia	247	18	15	10	1	1

[a] N, number of cones; R_a, mean nearest neighbor distance (unscaled); SD, standard deviation; S, separation distance; C_{sig}, number of subgroups with significant linear correlations; $C_{0.95}$, number of subgroups with strong linear correlations, defined as $r^2 > 0.95$.

possibly by topographic variability. Thus tubes or preferred pathways did not persist long enough to cause any significant nonrandom patterns (such as linear alignments) of tumuli and, by extension, of rootless cones. This would indicate a non-lava pathway control on cone formation in these cases, such as substrate hydrology.

5.2. Substrate Hydrology as Controlling Factor on Rootless Cone Distribution?

[28] It is unclear whether volatile distribution is uniform in the waterlogged substrate. If the substrate hydrology were originally uniform, cone formation in any given location would deplete the local subsurface volatile supply, deterring cones from forming near existing cones. This is the opposite of what is observed: Each RCG studied revealed significant (nonrandom) cone clustering. Thus a uniform substrate hydrology would suggest that the nonrandom spatial distribution of rootless cones is controlled by the location of preferred lava pathways. If, however, the substrate volatile distribution were not uniform, this in itself could explain the cone aggregation observed in nearest neighbor analysis: Cones could preferentially form in water-enriched areas. This explanation may be particularly appropriate for those RCGs lacking linear alignments (e.g., Raudholar).

6. Conclusions

[29] Our analysis shows that a record of preferred lava pathways and/or subsurface volatile distribution is preserved in the spatial distribution of Icelandic rootless cone groups. Despite appearances, Icelandic rootless cones are not randomly distributed within their respective cone groups; instead, they preferentially form near existing cones. The presence of at least one significant linear cone alignment in each RCG (and strong linear alignments in some groups) suggests that rootless cones form as the surface signature of preferred lava pathways. Nonuniform substrate volatile distribution may also be important, particularly in those RCGs that do not express pronounced linear alignments.

[30] We have shown that a statistical analysis of variance can be used to compare and contrast RCGs on Mars and Earth, thus providing a basis for developing inferences about conditions of formation when in situ study is not possible. An ANOVA on mean nearest neighbor distances reveals Martian candidate RCGs to be statistically indistinguishable from the Icelandic RCGs, supporting their candidacy as rootless cone groups. A similar ANOVA showed that the Martian cone groups do not resemble impact crater clusters: The impact craters have significantly greater nearest neighbor distances and show no evidence of aggregation within a crater group. Linear alignment detection analysis showed similar results for the Icelandic and Martian cone groups, again suggesting a rootless (hydrovolcanic) origin for the Martian cones.

7. Future Work

[31] Although we have shown striking similarities between the Icelandic RCGs and the Martian cone groups, we have not proven that the Martian cone groups are rootless. In particular, we cannot rule out other possible origins of the Martian cone groups, such as primary volcanic cones or pingos. Future work involves characterizing the nearest neighbor distributions of both primary volcanic cones and pingos on Earth and comparing these results to those of the

Figure 10. Linear alignment detection analysis results. Subgroups with statistically significant linear correlations are fit with lines; the cones in these subgroups are shown as either large dark squares ($r^2 > 0.95$) or pluses ($r^2 < 0.95$). (a) Landbrot RCG (Iceland). Twenty-three cone subgroups have significant linear correlations. The four subgroups with the strongest linear correlations (all $r^2 > 0.95$) are circled. These four lines are subparallel and may reflect the local lava flow direction. Cones that are not in these 23 subgroups are shown as light squares. (b) Raudholar RCG (Iceland). Linear cone alignments are largely absent, with only one cone subgroup found to have a significant linear correlation. (c) Cerberus Plains 1 candidate RCG (Mars). Four cone subgroups have significant linear correlations. Again, note their subparallel alignment.

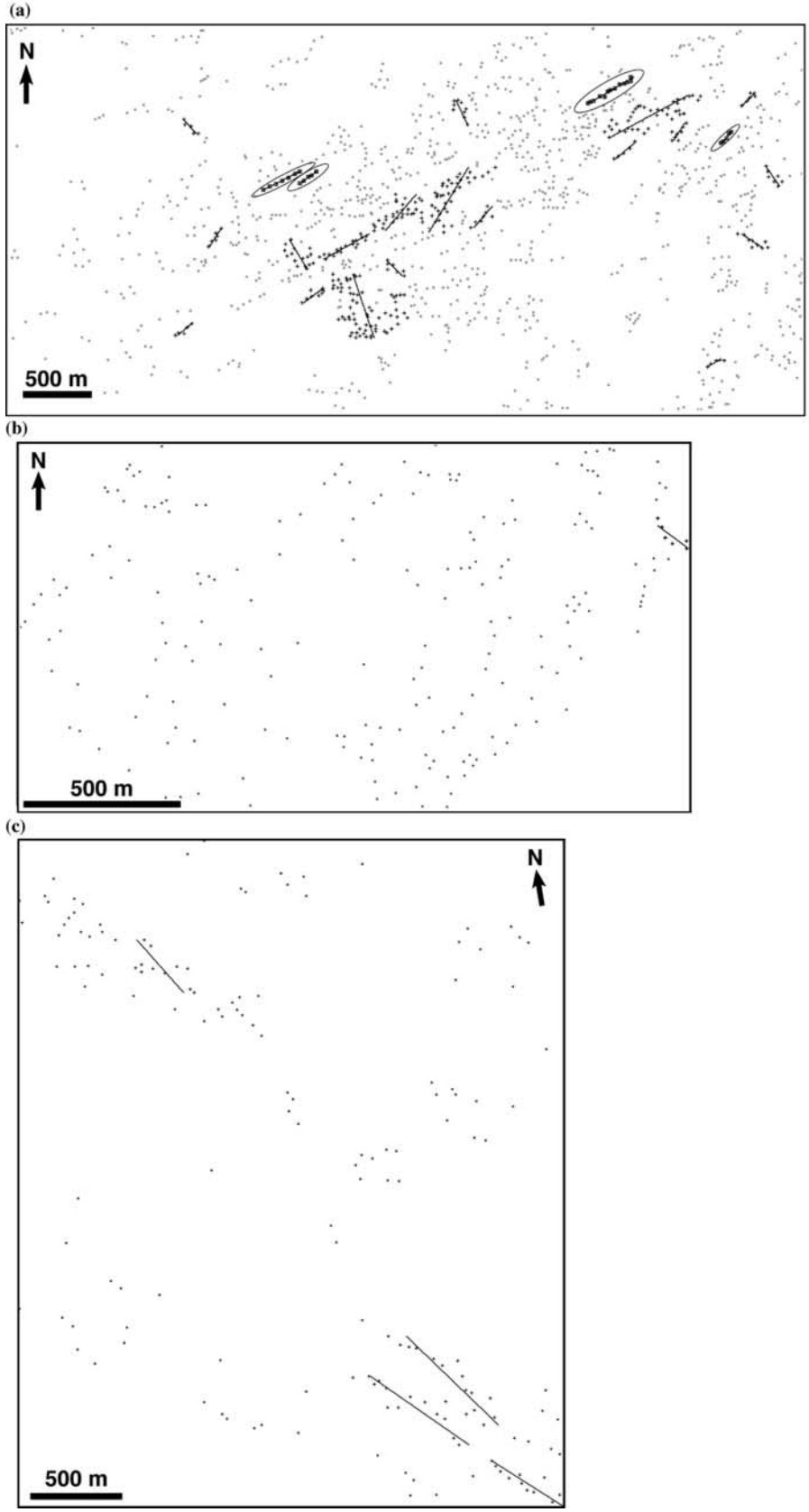

Figure 10

Martian cone groups. We will also analyze the spatial distribution of enigmatic, cone-like features on Mars (e.g., in the Athabasca Valles region). Finally, we will expand our linear analysis detection methodology to quantify any preferred directionality in the data.

[32] **Acknowledgments.** We are extremely grateful to L. Keszthelyi, A. McEwen, and P. Lanagan for their thorough, thoughtful reviews, which resulted in a significantly improved manuscript. L. Glaze and A. Duncan kindly provided copies of their manuscripts in advance of publication. This research was supported by NASA grant NAG5-13458. This paper is HIGP publication number 1337 and SOEST publication number 6407.

References

Allen, C. C. (1980), Volcano-ice interactions on the Earth and Mars, in *Reports of the Planetary Geology and Geophysics Program*, *NASA Tech. Memo., TM-81979*, 161–264.

Anderson, S. W., E. R. Stofan, S. E. Smrekar, J. E. Guest, and B. Wood (1999), Pulsed inflation of pahoehoe lava flows: Implications for flood basalt emplacement, *Earth Planet. Sci.*, *168*, 7–18.

Bruno, B. C., S. A. Fagents, T. Thordarson, and S. Baloga (2004), Spatial analysis of rootless cone groups on Iceland and Mars, *Lunar Planet. Sci. Conf. XXXIV*, Abstract 1368.

Clark, P. J., and F. C. Evans (1954), Distance to nearest neighbor as a measure of spatial relationships in populations, *Ecology*, *35*, 445–453.

Duncan, A. M., J. E. Guest, E. R. Stofan, S. W. Anderson, H. Pinkerton, and S. Calvari (2004), Development of tumuli in the medial portion of the 1983 aa flow field, Mount Etna, Sicily, *J. Volcanol. Geotherm. Res.*, *132*, 173–187.

Fagents, S. A., and T. Thordarson (2004), Rootless volcanic cones in Iceland and on Mars, in *The Geology of Mars: Evidence from Earth-Based Analogues*, chap. 8, edited by M. Chapman, Cambridge Univ. Press, New York, in press.

Fagents, S. A., P. D. Lanagan, and R. Greeley (2002), Rootless cones on Mars: A consequence of lava–ground ice interaction, in *Volcano-Ice Interaction on Earth and Mars*, edited by J. L. Smellie and M. G. Chapman, *Geol. Soc. Spec. Publ. London*, *202*, 295–317.

Frey, H., and M. Jarosewich (1982), Subkilometer Martian volcanoes: Properties and possible terrestrial analogs, *J. Geophys. Res.*, *87*, 9867–9879.

Frey, H., B. L. Lowry, and S. A. Chase (1979), Pseudocraters on Mars, *J. Geophys. Res.*, *84*, 8075–8086.

Glaze, L. S., S. W. Anderson, E. R. Stofan, S. Baloga, and S. E. Smrekar (2004), Statistical distribution of inflation features on lava flows: Analysis of flow surfaces on Earth and Mars, *Geol. Soc. Am. Bull*, in press.

Greeley, R., and S. A. Fagents (2001), Icelandic pseudocraters as analogs to some volcanic cones on Mars, *J. Geophys. Res.*, *106*, 20,527–20,546.

Guest, J. E., D. K. Chester, and A. M. Duncan (1984), The Valle del Bove, Mount Etna: Its origin and relation to the stratigraphy and structure of the volcano, *J. Volcanol. Geotherm. Res.*, *21*, 1–23.

Hodges, C. A., and H. J. Moore (1994), *Atlas of Volcanic Landforms on Mars*, *U.S. Geol. Surv. Prof. Pap.*, *1534*, 194 pp.

Lanagan, P. D., A. S. McEwen, L. P. Keszthelyi, and T. Thordarson (2001), Rootless cones on Mars indicating the presence of shallow equatorial ground ice in recent times, *Geophys. Res. Lett.*, *28*, 2365–2368.

Self, S., L. Keszthelyi, and T. Thordarson (1998), The importance of pahoehoe, *Annu. Rev. Earth Planet. Sci.*, *26*, 81–110.

Thorarinsson, S. (1951), Laxargljufur and Laxarhraun: A tephrochronological study, *Geogr. Ann.*, *H1–H2*, 1–89.

Thorarinsson, S. (1953), The crater groups in Iceland, *Bull. Volcanol.*, *14*, 3–44.

Thordarson, T. (2000), Rootless eruptions and cone groups in Iceland: Products of authentic explosive water to magma interactions, in *Volcano/Ice Interactions on Earth and Mars, Abstract Volume*, edited by V. C. Gulick and M. T. Gudmundsson, p. 48, Univ. of Iceland, Reykjavik.

Thordarson, T., and A. Hoskuldsson (2002), *Iceland*, 200 pp., Terra Publ., Hertfordshire, UK.

Thordarson, T., et al. (1992), Origins of rootless cone complexes in S. Iceland, in *The 20th Nordic Geological Winter Meeting*, edited by A. Geirsdóttir, H. Norddahl, and G. Helgadóttir, p. 169, Icelandic Geol. Soc., Reykjavik.

Thoroddsen, T. (1894), Ferd un vestur Skaftafellssyslu sumarid 1893 (Travelogue from western Skaftafellshire in the summer of 1893), *Andvari*, *19*, 44–161.

S. M. Baloga, Proxemy Research, 14300 Gallant Fox Lane, Suite 225, Bowie, MD 20715, USA. (steve@higp.hawaii.edu)

B. C. Bruno, S. A. Fagents, and E. Pilger, Hawaii Institute of Geophysics and Planetology, University of Hawaii at Manoa, 2525 Correa Road, Honolulu, HI 96822, USA. (bruno@higp.hawaii.edu; fagents@higp.hawaii.edu; pilger@higp.hawaii.edu)

T. Thordarson, Department of Geology and Geophysics, University of Hawaii at Manoa, 2525 Correa Road, Honolulu, HI 96822, USA. (moinui@soest.hawaii.edu)